Light polarization measurements in tests of macrorealism

Eugenio Roldán,[1,2] Johannes Kofler,[2] and Carlos Navarrete-Benlloch[2,3,4]

[1]*Departament d'Òptica i d'Optometria i Ciències de la Visió,*
Universitat de València, Dr. Moliner 50, 46100 Burjassot, Spain.
[2]*Max-Planck-Institut für Quantenoptik, Hans-Kopfermann-strasse 1, 85748 Garching, Germany.*
[3]*Max-Planck-Institut für die Physik des Lichts, Staudtstrasse 2, 91058 Erlangen, Germany.*
[4]*Institute for Theoretical Physics, Erlangen-Nürnberg Universität, Staudtstrasse 7, 91058 Erlangen, Germany.*

According to the world view of macrorealism, the properties of a given system exist prior to and independent of measurement, which is incompatible with quantum mechanics. Leggett and Garg put forward a practical criterion capable of identifying violations of macrorealism, and so far experiments performed on microscopic and mesoscopic systems have always ruled out in favor of quantum mechanics. However, a macrorealist can always assign the cause of such violations to the perturbation that measurements effect on such small systems, and hence a definitive test would require using non-invasive measurements, preferably on macroscopic objects, where such measurements seem more plausible. However, the generation of truly macroscopic quantum superposition states capable of violating macrorealism remains a big challenge. In this work we propose a setup that makes use of measurements on the polarization of light, a property which has been extensively manipulated both in classical and quantum contexts, hence establishing the perfect link between the microscopic and macroscopic worlds. In particular, we use Leggett-Garg inequalities and the criterion of no-signaling in time to study the macrorealistic character of light polarization for different kinds of measurements, in particular with different degrees of coarse-graining. Our proposal is non-invasive for coherent input states by construction. We show for states with well defined photon number in two orthogonal polarization modes, that there always exists a way of making the measurement sufficiently coarse-grained so that a violation of macrorealism becomes arbitrarily small, while sufficiently sharp measurements can always lead to a significant violation.

I. INTRODUCTION

In 1985, Leggett and Garg introduced the concept of macroscopic realism (macrorealism) [1, 2]. According to this worldview, macroscopic objects are always in a state with well defined properties and measurements can be performed without changing these properties and the subsequent temporal evolution. If effects of decoherence can be sufficiently suppressed, quantum mechanics is at variance with macrorealism. While experiments with genuine macroscopic objects ("Schrödinger cats") have not been performed yet, the past few years have demonstrated that quantum mechanics still prevails for mesoscopic objects [3–8].

Leggett-Garg inequalities (LGIs) can witness a violation of macrorealism by suitably comparing correlations of a dichotomized observable that is measured at subsequent times under different measurement settings. The concept of non-invasive measurability is essential for their derivation: provided that the disturbance on the target system is negligibly small during the measurement, the violation of a LGI would imply that the corresponding observable does not obey macrorealism. Recently, an alternative criterion for macrorealism called no-signaling in time (NSIT) [9] has been put forward, which is now known to be in general stronger than LGIs [10], providing not only sufficient but also necessary conditions for the absence of macrorealism [11].

While the preparation of exotic quantum states such as macroscopic spatial superpositions remains one of today's most anticipated challenges in quantum mechanics

[12–16], the polarization of light, with a long experimental history both in classical and quantum physics, offers a perfect property where studying macrorealism. Experiments have indeed been performed with single photons in a superposition of two orthogonal polarization states [17], following closely the original Leggett-Garg proposal. Although it is widely accepted that the results of this study are in favor of quantum mechanics, they seem to suggest that violations of macrorealism weaken as the measurements are made less invasive, and the biggest violations are found whenever the weak values are *strange*. In addition, violations of macrorealism can be traced back in this case directly to the superposition of the two orthogonal polarizations. In this work we consider a different setup, involving (strong) measurements whose invasiveness can be varied in two different ways, and which allow for violations of macrorealism for a broader type of states, including some which make no apparent use of the superposition principle.

As explained in detail below, starting from a well defined spatiotemporal mode of the light field, we propose using (polarization-insensitive) beam splitters to perform photon counting measurements of the reflected beam's polarization. Since coherent states remain coherent after the beam splitter, the setup doesn't change the polarization state for such states, and hence it can be regarded as non-invasive in the classical limit. In addition, it is shown that the measurements preserve the polarization state when the initial state is pure and has well-defined polarization. It follows that a requirement for violations of macrorealism in our setup is the presence of quantum states with a degree of polarization smaller than one,
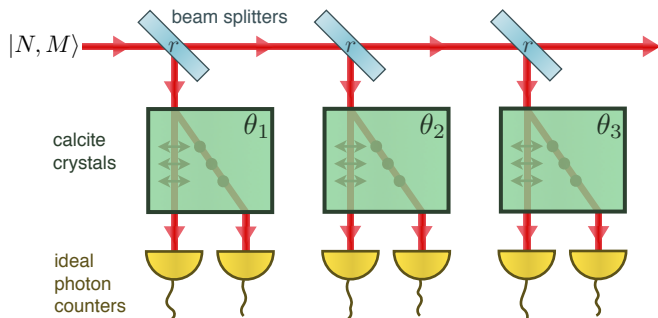
FIG. 1. Sketch of the measurement protocol. Light pulses (following the red path) are prepared in a state with well defined photon numbers in the x and y linear polarizations. Each detection port acts following the same three steps: (i) the pulses go through a beam splitter with reflectivity r, (ii) their polarization components with respect to some linear basis defined by an angle θ_p are separated with a calcite crystal or any other method of choice, and (iii) finally the photon number is measured on each polarization. Violations of macrorealism can be then checked by studying the correlations between measurements on the different ports.

which is a broader condition than having superpositions of different polarization states.

For definiteness, we concentrate on linear polarization states with well-defined photon number, even if some comments will be made about other types of states. We pay special attention to the influence of the type of measurements, as we consider measurements consisting in the extraction of a fixed number of photons, but also measurements that average over the number of detected photons. Our work can be seen then as a study about the invasiveness of polarization measurements via photon subtraction, and sheds light onto the question under which measurement conditions a violation of macrorealism can be observed. Our results are in agreement with earlier studies which show that, for most time evolutions, sufficiently coarse-grained measurements do not show a violation of macrorealism while sufficiently sharp measurements do [11, 18–21].

II. THE PROTOCOL

Consider a source of quantum light emitting a sequence of identical pulses traveling along the z direction, in a well defined transverse spatial mode. Each pulse is prepared in a state with N and M photons linearly polarized along the x and y directions, respectively, a state denoted by $|N, M\rangle$. The pulses travel through three detection ports which act exactly in the same way, see Fig. 1. A fraction of the input light is extracted via a beam splitter of (polarization-independent) reflectivity r, which will be considered infinitesimally small when aiming for a non-invasive measurement, although we will also study the effect of larger reflectivity values. This small amount of reflected light is then split into its orthogonal linear po-

larization components with respect to some θ–oriented reference frame (this can be accomplished, e.g., by a properly oriented calcite crystal), and each of the two orthogonally polarized beams impinge on ideal photon counters that we denote by x and y detectors. We assume that the reflectivity r is the same for all the detection ports, while they might differ in the polarization angles θ. In order to study LGIs and NSIT, one must analyze correlations between the statistics of the measurements at the different detection ports, as we explain in detail below.

Note that each port allows performing a measurement of the polarization state of the reflected beam, since accumulating the measurement results pulse after pulse to determine the probability distributions at the photon counters, one can unveil the statistics of the Stokes parameters (when measuring along two different polarization orientations). It is easy to show that the statistics of the Stokes parameters are the same for the reflected and input beams for coherent and thermal states (making the device a practical one for measuring the polarization state of classical light), which is also true for Fock states at least for first and second order moments.

Let us now explain how do we dichotomize the measurement outcomes. The detectors are capable of counting photons, and hence in principle they will provide outcomes $\omega_x = 0, 1, 2, ...$ and $\omega_y = 0, 1, 2, ...$, where the subindex labels the detector. We consider different strategies to dichotomize these outcomes, all requiring post-selection and based on some kind of "majority vote", that is, which detector has detected more photons:

(a) $\mathcal{S}$ (sharp) measurements, in which one of the detectors doesn't click, but the other measures some given number of photons $\omega \geqslant 1$ that we choose. Hence, we post-select to events with either $(\omega_x = \omega, \omega_y = 0)$ or $(\omega_x = 0, \omega_y = \omega)$. In the first case we say that the outcome corresponds to an *x-event*, while it is a *y-event* in the second case. We will use the notation $\mathcal{S}_\omega$ whenever we want to refer explicitly to the value of ω that we chose.

(b) $\mathcal{F}$ (fair) measurements, in which we keep all the outcomes up to some maximum value $\omega_{\max}$ in both detectors. Any outcome in which the x detector has measured more photons than the y detector is characterized as an x-event, and vice versa, outcomes in which the y detector has measured more photons than the x detector are characterized as a y-event. As with the previous type, we will use the notation $\mathcal{F}_{\omega_{\max}}$ when needed.

(c) $\mathcal{B}$ (blurred, or intermediate) measurements, in which only outcomes from a certain photon-number interval $[\omega_{\min}, \omega_{\max}]$ are considered, and the dichotomization is performed as in the previous case. When in need of being more explicit, we will denote these measurements by $\mathcal{B}_{[\omega_{\min}, \omega_{\max}]}$. Note that by taking $\omega_{\min} = 1$ we recover type $\mathcal{F}_{\omega_{\max}}$, while by taking $\omega_{\min} = \omega_{\max} = \omega$ we recover type $\mathcal{S}_\omega$.

The above types of measurements affect the incoming pulse in different ways. How invasive they are depends both on the beam splitter reflectivity r, as it limits the
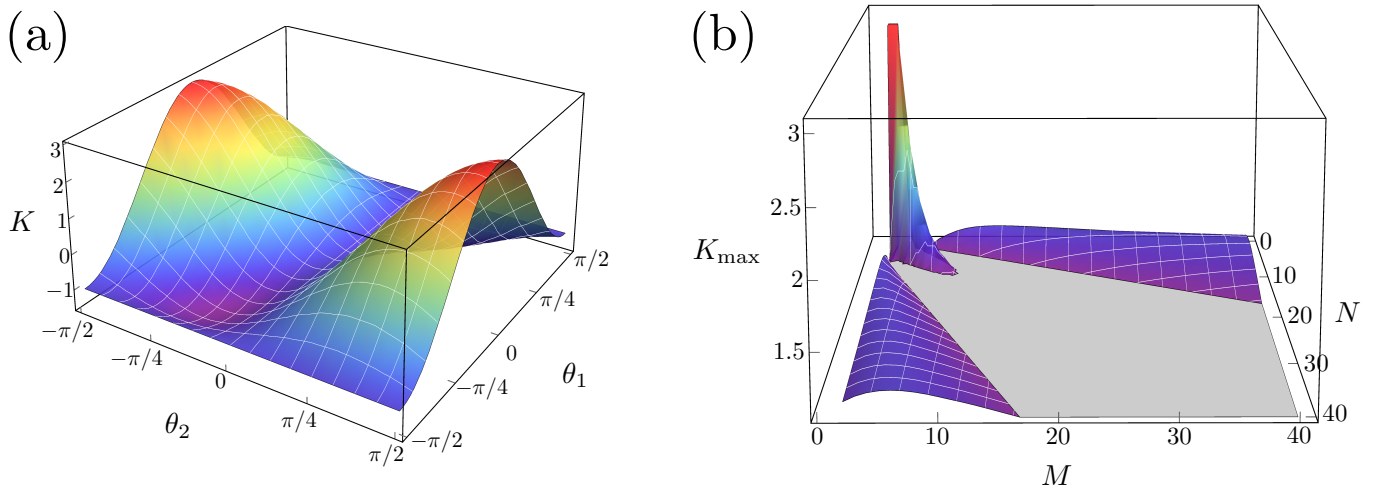
FIG. 2. (a) K as a function of θ_2 and θ_3 for $\theta_1 = \pi/2$ and for the state $|1,1\rangle$ and $\mathcal{S}_1$ measurements. For this type of measurements this is the only one that violates the LGI, and it does so maximally, as $K_{\max} = 3$. (b) $K_{\max}$ as a function of N and M for $\mathcal{S}_2$ measurements. The grey area marks the region where the LGI is preserved, and it can be appreciated that the violation remains for large values of N and M.

number of photons that can be extracted from the light beam, and on the choice of measurement, since these are "selective" in different degrees, in the sense that they make use of more or less likely events. The least invasive measurement would be one that is minimally reflecting and minimally selective, that is, it makes use of all the photon counts. The ideal non-invasive measurement corresponds then to an $\mathcal{F}_{\omega_{\max}}$ measurement satisfying the condition $(N + M)r^2 \ll 1 < \omega_{\max}$. Contrarily, the $\mathcal{S}$ type is the more selective, while the $\mathcal{B}$ type allows us to move in between the $\mathcal{F}$ and $\mathcal{S}$ types.

III. CRITERIA FOR VIOLATIONS OF MACROREALISM

In order to evaluate both the LGIs and NSIT, it is necessary to evaluate not only the probabilities $P_a(\theta)$ of having an a-event for a setting θ of the detector (in the following the indices a, b, and c take values from the event labels x and y), but also the conditional probabilities $P_{ab}(\theta_p, \theta_q)$ of having an a-event at one device with polarization angle $\theta = \theta_p$ followed by a b-event at a subsequent device with $\theta = \theta_q$ (in the following, the indices p and q take values from the measurement ports 1, 2, and 3), which we will denote as an ab-event. For NIST, we will also need to introduce abc-events, with associated probability $P_{abc}(\theta_1, \theta_2, \theta_3)$, related to three consecutive measurements performed over the same pulse (with measurement p at a polarization angle θ_p). The mathematical expressions for all these probabilities, as well as their detailed derivation within the quantum mechanical framework, can be found in the appendix. In the following we move directly to introducing our criteria for violations of macrorealism and discussing the results.

Let us now introduce the criteria based on LGIs and

NIST. The basic objects required to compute LGIs are the correlation functions between two measurement ports

$$C_{pq}(\theta_p, \theta_q, r) = \frac{P_{xx} + P_{yy} - P_{xy} - P_{yx}}{P_{xx} + P_{yy} + P_{xy} + P_{yx}}, \quad (1)$$

where we have included explicitly the dependence on the reflectivity coefficient of the beam splitters. Together with the type of measurement, and the number of photons N and M in the input state, these are all the variables that define the problem. Note that whenever $C_{pq} = +1\,(-1)$ the devices show perfectly correlated (anticorrelated) results. The LGI reads then [2]

$$K(\theta_1, \theta_2, \theta_3, r) = C_{12} + C_{23} - C_{13} \leq 1. \quad (2)$$

A convenient witness is obtained by maximizing this quantity over the polarization angles, defining then

$$K_{\max}(r) = \max_{\theta_1, \theta_2, \theta_3} K(\theta_1, \theta_2, \theta_3, r),$$

which witnesses a violation of the LGI (absence of macrorealism) whenever it is larger than 1 (note that it is upper-bounded by 3).

NSIT requires analyzing the disturbance effected by one measurement device on the others [9]. When only two consecutive measurements are considered, we then need to compare the probability distributions on the second device without and with a measurement in a previous device. These are given, respectively, by

$$\mathcal{P}_b(\theta_2) = \frac{P_b(\theta_2)}{\sum_a P_a(\theta_2)}, \quad (3a)$$

$$\mathcal{P}_b'(\theta_1, \theta_2) = \frac{\sum_a P_{ab}(\theta_1, \theta_2)}{\sum_{a,b} P_{ab}(\theta_1, \theta_2)}, \quad (3b)$$
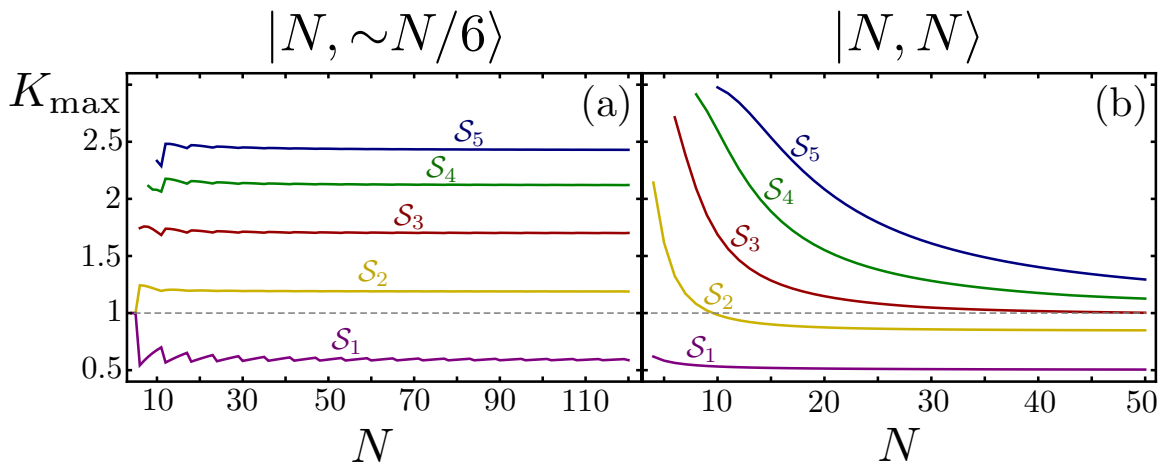
FIG. 3. $K_{\max}$ for states $|N, \sim N/6\rangle$ and $|N, N\rangle$ in (a) and (b), respectively, as a function of N for different types of $\mathcal{S}_\omega$ measurements (as indicated for each line).

which are both normalized probability distributions over the measurement outcomes of the second device, and can be compared via the Bhattacharyya coefficient

$$V_{(1)2} = \min_{\theta_1, \theta_2} \sum_{b=x,y} \sqrt{\mathcal{P}_b(\theta_2)\, \mathcal{P}'_b(\theta_1, \theta_2)}, \qquad (4)$$

which we minimize over the polarization angles, as we did with for criterion based on LGIs. Note that whenever the probability distributions are equal, $V_{(1)2} = 1$ and the measurement on the first device has no effect on the second. If that's not the case, then $V_{(1)2} < 1$. When three consecutive measurements are considered, then one also needs to consider the joint probability distribution of two devices, without and with the presence of a previous measurement; these are given, respectively, by

$$\mathcal{P}_{bc}(\theta_2, \theta_3) = \frac{P_{bc}(\theta_2, \theta_3)}{\sum_{b,c} P_{bc}(\theta_2, \theta_3)}, \qquad (5a)$$

$$\mathcal{P}'_{bc}(\theta_1, \theta_2, \theta_3) = \frac{\sum_a P_{abc}(\theta_1, \theta_2, \theta_3)}{\sum_{abc} P_{abc}(\theta_1, \theta_2, \theta_3)}, \qquad (5b)$$

and are again compared via the minimized Bhattacharyya coefficient

$$V_{(1)23} = \min_{\theta_1, \theta_2, \theta_3} \sum_{b,c} \sqrt{\mathcal{P}_{bc}(\theta_2, \theta_3)\, \mathcal{P}'_{bc}(\theta_1, \theta_2, \theta_3)}. \qquad (6)$$

In all cases NSIT requires $V = 1$ [9], so that $V < 1$ witnesses a violation, and hence absence of macroscopic realism in favor of quantum mechanics.

IV. RESULTS

In this section we summarize the main results found through an extensive numerical analysis based on the expressions provided in the appendix. We present them in two subsections. We start with $\mathcal{S}$ measurements, and then follow with $\mathcal{B}$ and $\mathcal{F}$ measurements. We discuss the results assuming $N \geq M$ for concreteness, but the results are invariant under the exchange $N \leftrightarrow M$.

A. $\mathcal{S}$ measurements

A common trait to $\mathcal{S}_\omega$-type measurements is that the results do not depend on the reflectivity r for any choice of ω. In particular, the reflectivity appears only as a prefactor in the different absolute probabilities P_a, P_{ab}, and P_{abc}, which disappears once we consider normalized objects such as correlations C_{pq} or probability distributions $\mathcal{P}_a$, $\mathcal{P}'_a$, $\mathcal{P}_{ab}$, and $\mathcal{P}'_{ab}$.

Let us first consider $\mathcal{S}_1$ measurements. It turns out that there is a single Fock state that violates the LGI, namely state $|1, 1\rangle$, for which K is shown in Fig. 2(a) as a function of θ_1 and θ_2 for $\theta_3 = \pi/2$. Notice that the violation is maximal as $K_{\max} = 3$. Regarding NSIT, it turns out that $V_{(1)2} = V_{(1)23} = 1$ for all angles $(\theta_1, \theta_2, \theta_3)$ and for all Fock states $|N, M\rangle$. Hence the violation of the LGI by the state $|1, 1\rangle$ is not captured by $V_{(1)2}$ (note that for state $|1, 1\rangle$ it does not make any sense to think about $V_{(1)23}$ as there are not enough photons for three detections).

The results are very different for $\mathcal{S}_{\omega > 1}$ measurements. In this case, there are an infinite number of states that violate both the LGIs and NSIT for each ω. Let us first consider LGIs. In Fig. 2(b) we show $K_{\max}$ as a function of N and M for $\omega = 2$. It can be appreciated that states with $1 \lesssim M < M_{\max} \sim 0.4N$ have $K_{\max} > 1$. Hence the domain of states that violate the LGI in $\mathcal{S}_{\omega > 1}$ measurements is not bounded for large values of N. For a given N we have found by inspection that the states with $M \sim N/6$ are the ones exhibiting a larger violation, with a $K_{\max}$ quickly arriving to an asymptotic value as N increases, as shown in Fig. 3(a) for several values
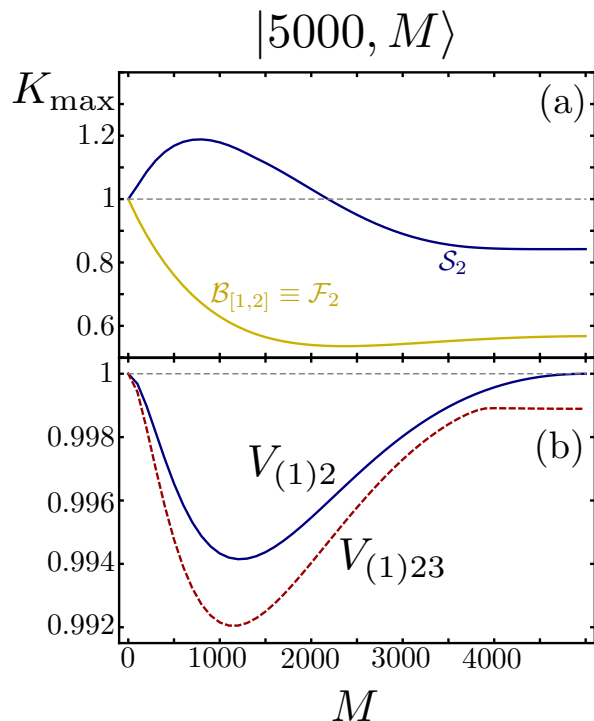
FIG. 4. (a) $K_{\max}$ for states $|5000, M\rangle$ as function of M for two types of measurements, $\mathcal{S}_2$ and $\mathcal{F}_2$ (with $r = 0.1$ for the last one). (b) Bhattacharyya coefficients $V_{(1)2}$ and $V_{(1)23}$ for the same states as a function of M subject to $\mathcal{S}_2$ measurements.

of ω. Contrarily, for states with $M > M_{\max}$ there is an upper value of N beyond which the violation of the LGI disappears, which is illustrated for states $|N, N\rangle$ in Fig. 3(b). This last result suggests that superpositions of $|N, N\rangle$ states could violate LGIs only provided N is not too large, which could be illustrated with the experimentally accessible two-mode squeezed vacuum states.

Let us now move to NSIT. We have found $V_{(1)2} = 1$ for all states $|N, N\rangle$ and $|N, 0\rangle$, independently of N and the choice of angles (θ_1, θ_2). For the rest of Fock states, $V_{(1)2}$ is smaller than one for small photon numbers, but rapidly grows towards an asymptotic value close to one, which is typically reached for photon numbers around 100. The behavior of $V_{(1)23}$ is different, as only states $|N, 0\rangle$ have $V_{(1)23} = 1$.

In Figs. 4 we illustrate this conclusions by considering the states $|N = 5000, M\rangle$, plotting different quantities as a function of M for $\mathcal{S}_2$ measurements. We show $K_{\max}$ in Fig. 4(a), which shows a maximum at $M \sim 800 \sim 5000/6$ as expected. In Fig. 4(b) we show $V_{(1)2}$ and $V_{(1)23}$, where we can appreciate that $V_{(1)2} = 1$ for $M = 0$ and $M = 5000$, while $V_{(1)23} = 1$ only for $M = 0$, both quantities being smaller than one for any other M.

In summary, using $\mathcal{S}_{\omega>1}$ measurements both NSIT and LGIs are violated by an infinite number of states, the violation being larger for larger ω, consistent with the fact that the measurement becomes increasingly selective. The exceptions are completely polarized states

(those with $M = 0$), for which no violation of macroscopic realism is found, as expected from the fact that our photon subtraction scheme cannot change their polarization state.

Let us remark that, while it might seem surprising the abrupt change in the the number of states which violate macrorealism when moving from $\mathcal{S}_1$ to $\mathcal{S}_{\omega>1}$ measurements, these are indeed two very different types of measurements. In the first case, one is really post-selecting to the most likely events (reflection of a single photon), while in the second case, one post-selects to increasingly unlikely events (reflection of many photons). Hence, compared to $\mathcal{S}_1$ measurements, $\mathcal{S}_{\omega>1}$ measurements are extremely selective, and therefore, extremely invasive.

B. $\mathcal{B}$ and $\mathcal{F}$ measurements

In contrast to $\mathcal{S}$ measurements, for the $\mathcal{B}$ and $\mathcal{F}$ types the results depend on the reflectivity, as we discuss next.

As an initial example, in Fig. 4(a) we consider a $\mathcal{B}_{[1,2]}$ measurement (which is as well an $\mathcal{F}_2$ measurement), showing how the violations of the LGI which we found for $\mathcal{S}_2$ measurements are completely smeared off when single photon detections are also considered.

Let us now consider more complex measurements with $\omega_{\max} = 4$ and study the effect of how selective the measurement is, focusing on states with $M \sim N/6$, which we have found to be the ones violating the LGI the strongest for $\mathcal{S}_{\omega>1}$ measurements. For $\mathcal{S}_4$ measurements we saw that $K_{\max}$ reaches an asymptotic value above 1 as the photon number N is increased. In contrast, $\mathcal{B}_{[1<\omega_{\min}<4,4]}$ measurements do not show such an asymptote, and indeed $K_{\max}$ becomes smaller than 1 above some critical photon number N_c. In Fig. 5 we represent N_c as a
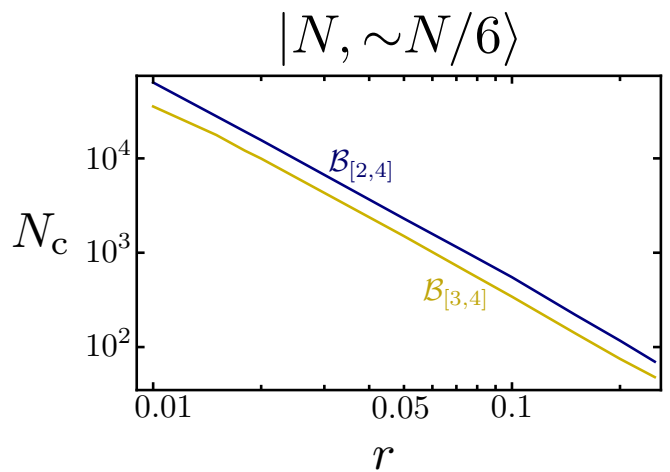

FIG. 5. Critical value N_c of the photon number above which violations of LGI disappear as a function of the reflectivity r for states of the type $|N, \sim N/6\rangle$ and the types of $\mathcal{B}$ measurements indicated in the figure. Notice the logarithmic scale in both axes.
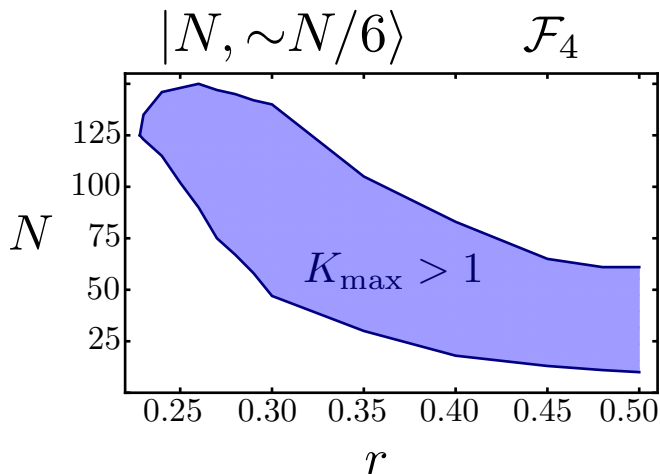
FIG. 6. Region of violation of the LGI in the (N, r) parameter space for states of the $|N, \sim N/6\rangle$ type and $\mathcal{F}_4$ measurements.

FIG. 7. Bhattacharyya coefficients $V_{(1)2}$ and $V_{(1)23}$ as a function of M for states $|5000, M\rangle$ and $\mathcal{F}_2$ measurement. We set $r = 0.01$.

function of the reflectivity r for $\mathcal{B}_{[3,4]}$ and $\mathcal{B}_{[2,4]}$ measurements, showing that coarse graining works against the violation of macrorealism, that is, N_c is smaller the smaller $\omega_{\min}$ is. The results are similar for $\mathcal{F}_4$ measurements, that is, there is a critical value of N beyond which there is no violation of the LGI, but in such case there are also certain values of N and the reflectivity below which $K_{\max} < 1$. We illustrate this in Fig. 6, where the condition $K_{\max} > 1$ is shown to lead to a closed domain in the space of parameters (r, N).

As for NSIT, our numerical analysis shows that it is violated for all states except $|N, 0\rangle$, but the violation is weakened as the range $[\omega_{\min}, \omega_{\max}]$ is increased or the reflectivity r is reduced. As an example, in Fig. 7 we show $V_{(1)2}$ and $V_{(1)23}$ as a function of M for states $|N = 5000, M\rangle$ and a $\mathcal{B}_{[1,2]}$ (which, we remark again, is an $\mathcal{F}_2$ measurement as well). The shape of the curves is essentially the same as for $\mathcal{S}_2$ measurements, see Fig. 5(b), but their peak values are much closer to one, and hence the violation of macrorealism is weakened.

V. DISCUSSION AND CONCLUSIONS

Let us finally offer some conclusions that can be drawn from the results presented above and comment on possible future work.

Probably the most interesting question that our results might give an answer to is: has the polarization of light a macrorealistic character? In the setup we studied, the answer seems to be positive, because violations of macrorealism are weakened as the invasiveness of the measurements is reduced, that is, as we approach the condition $(N + M)r^2 \ll 1 < \omega_{\max}$. This conclusion is in agreement with the previous experimental analysis that we commented on in the introduction [17].

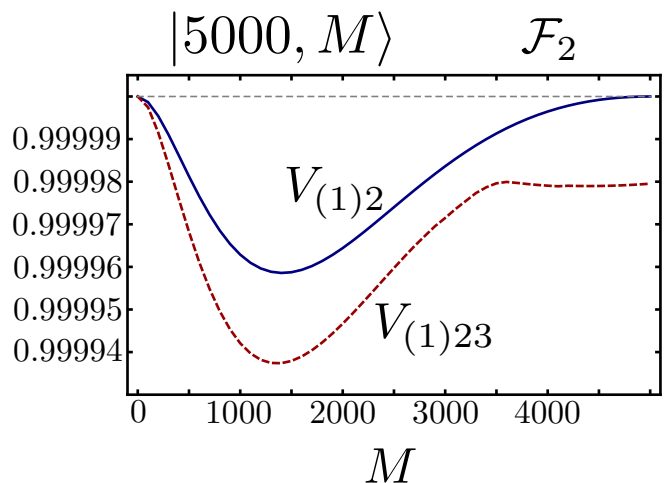A complementary question that our work answers as

well is: does quantum mechanics allow for a truly non-invasive way of measuring the polarization of light? Recall that our setup is indeed capable of reconstructing the statistics of the Stokes parameters, and hence the polarization state. Hence, we can conclude that truly non-invasive polarization measurements in the macroscopic domain occur only for $\mathcal{S}_1$ measurements (i.e., removing single photons), as NSIT is never violated, while LGIs are solely violated by the state $|1, 1\rangle$, certainly not a macroscopic state. Any other type of measurement subtracting more photons disturbs the system enough as to have violations of macrorealism. However, we have also found that coarse-graining the measurements and increasing the system size (input number of photons) tends to make the violations disappear, so that polarization measurements may be regarded as asymptotically non-invasive in this limit as well.

Note that these conclusions are drawn both from the analysis of LGIs and NSIT. Hence, even though the conditions for macrorealism based on these criteria are inequivalent in general (as explained above, NSIT provides stronger conditions), in our setup both can be used interchangeably. Moreover, if instead of a sharp $V = 1$ macrorealism condition for the Bhattacharyya coefficients, one allows for an inequality type condition $V > V_0$ (with V_0 properly chosen for each type of measurement), we have checked that the NSIT conditions reproduce the results found with LGIs even quantitatively.

An interesting outlook that draws from our work is the analysis of other types of input states, particularly those which make use of the superposition principle. For example, considering GHZ states of the form $|N, 0\rangle + |0, N\rangle$, quantum mechanics predicts that even coarse-grained measurements would lead to a violation of macrorealism in certain setups [22, 23]. It will be interesting to analyze whether this is also the case in our setup, even when the measurements can be considered non-invasive,

opening then the possibility to rule out either macrorealism or quantum mechanics for the polarization degree of freedom of light.

Let us finally comment on a different type of input states that we have considered, which have the form $|\alpha\rangle \otimes |N\rangle$, that is, the mode polarized along the x direction is in a coherent state of amplitude α, while the one along the y direction is in a Fock state with N photons. This state is interesting because it is a combination of a classical and a quantum state. Preliminary results show that, for $\mathcal{S}$ measurements, the states that maximally violate LGIs have $|\alpha|^2 \sim N/6$, which is consistent with we showed in the previous section. However, in this case the dependence of $K_{\max}$ on the photon number $|\alpha|^2$ is not as strong as it was with Fock states. Moreover, the domain of angles where the violation occurred shrinks as $|\alpha|^2$ grows, in contrast with what happens for the Fock state $|N, \sim N/6\rangle$ for which the domain of violation in the angle space is N-independent. Hence, increasing the "classicality" of the state works agains violations of macrorealism, as expected.

Appendix A: Determination of probabilities

In this appendix we derive the expressions for the conditional probabilities appearing in the LGI and the NSIT conditions. We proceed by determining the unnormalized state of the system after obtaining a given outcome (photon counts) on each of the measurement ports. The norm of this state provides the probability of those particular outcomes.

1. First measurement

At each detection port, the pulses undergo a series of transformations: first, they mixed in a beam splitter with a vacuum state, then the polarization of the reflected pulse is rotated by an angle θ, and finally photon counters measure a given number of photons in the x and y polarizations of this pulse, so that the transmitted state gets projected to the corresponding outcome (although physically different, this is equivalent to the effect of the calcite crystal of Fig. 1, in which the two orthogonal linear polarizations along some angle θ are separated and photon-counted). Let us find the post-selected state now.

Consider an input state

$$|N, M\rangle = \frac{1}{\sqrt{N!M!}} \left(\hat{a}_x^\dagger\right)^N \left(\hat{a}_y^\dagger\right)^M |0\rangle, \qquad (A1)$$

where $\hat{a}_c^\dagger$ are creation operators for c-polarized photons. In the following we will denote by $|0\rangle$ the vacuum state of whatever number of modes we are dealing with. The action of the beam splitter is described [24] by the unitary operator $\hat{B}(r) = \exp(\alpha \hat{a}_x^\dagger \hat{b}_x + \alpha \hat{a}_y^\dagger \hat{b}_y - \text{H.c.})$, where $r = \cos\alpha$ and $t = \sin\alpha$ are the reflectivity and transmissivity of the beam splitter, and $\hat{b}_c$ are the annihilation operators for the second port. Applying this operator to the input state, including the vacuum state for the modes of the second port, we obtain

$$|\psi_1\rangle = \hat{B}(r) |N, M\rangle \otimes |0\rangle \qquad (A2)$$

$$= \frac{1}{\sqrt{N!M!}} \left(t\hat{a}_x^\dagger + r\hat{b}_x^\dagger\right)^N \left(t\hat{a}_y^\dagger + r\hat{b}_y^\dagger\right)^M |0\rangle$$

$$= \frac{t^{N+M}}{\sqrt{N!M!}} \sum_{n=0}^{N} \sum_{m=0}^{M} \left(\frac{r}{t}\right)^{n+m} \binom{N}{n}\binom{M}{m}$$

$$\times \left(\hat{a}_x^\dagger\right)^{N-n} \left(\hat{a}_y^\dagger\right)^{M-m} \left(\hat{b}_x^\dagger\right)^n \left(\hat{b}_y^\dagger\right)^m |0\rangle.$$

The rotation of the polarization of the reflected modes is described by the unitary operator $\hat{R}(\theta) = \exp(\theta \hat{b}_x^\dagger \hat{b}_y - \text{H.c.})$. We will denote the shorthand notation $s = \sin\theta$ and $c = \cos\theta$ in what follows. Applying this transformation to the previous state we obtain

$$|\psi_2\rangle = \hat{R}(\theta) |\psi_1\rangle \qquad (A3)$$

$$= \frac{t^{N+M}}{\sqrt{N!M!}} \sum_{n=0}^{N} \sum_{m=0}^{M} \left(\frac{r}{t}\right)^{n+m} \binom{N}{n}\binom{M}{m} \left(\hat{a}_x^\dagger\right)^{N-n}$$

$$\times \left(\hat{a}_y^\dagger\right)^{M-m} \underbrace{\left(c\hat{b}_x^\dagger - s\hat{b}_y^\dagger\right)^n \left(s\hat{b}_x^\dagger + c\hat{b}_y^\dagger\right)^m |0\rangle}_{|0\rangle \otimes |\mathcal{Z}_{nm}(\theta)\rangle},$$

Suppose that the photon-counters detect ω_x and ω_y photons in the corresponding mode. Defining the Fock-basis projector $\hat{\Pi}_{\omega_x\omega_y} = |\omega_x\rangle\langle\omega_x| \otimes |\omega_y\rangle\langle\omega_y|$, the state of the transmitted modes is finally transformed [24] into the (un-normalized) state $\text{tr}_b\{(\hat{I} \otimes \hat{\Pi}_{\omega_x\omega_y}) |\psi_2\rangle\langle\psi_2|\} = |\varphi\rangle\langle\varphi|$, with

$$|\varphi\rangle = \frac{t^{N+M}}{\sqrt{N!M!}} \sum_{n=0}^{N} \sum_{m=0}^{M} \left(\frac{r}{t}\right)^{n+m} \binom{N}{n}\binom{M}{m} \qquad (A4)$$

$$\times \left(\hat{a}_x^\dagger\right)^{N-n} \left(\hat{a}_y^\dagger\right)^{M-m} \langle\omega_x, \omega_y |\mathcal{Z}_{nm}(\theta)\rangle |0\rangle.$$

Let us evaluate $\langle\omega_x, \omega_y |\mathcal{Z}_{nm}(\theta)\rangle$ separately, for which we first rewrite

$$|\mathcal{Z}_{nm}(\theta)\rangle = \sum_{i=0}^{n} \sum_{j=0}^{m} (-1)^i \binom{n}{i}\binom{m}{j} c_\theta^{n-i+j} s_\theta^{m+i-j} \qquad (A5)$$

$$\times \left(\hat{b}_x^\dagger\right)^{n+m-i-j} \left(\hat{b}_y^\dagger\right)^{i+j} |0\rangle,$$

and then calculate

$$
\begin{aligned}
\langle \omega_x, \omega_y \, | \mathcal{Z}_{nm}(\theta) \rangle &= \sum_{i=0}^{n} \sum_{j=0}^{m} (-1)^i \binom{n}{i} \binom{m}{j} c^{n-i+j} s^{m+i-j} \\
&\quad \times \sqrt{(n+m-i-j)! \, (i+j)!} \qquad \text{(A6)} \\
&\quad \times \underbrace{\langle \omega_x \, | n+m-i-j \rangle}_{\delta_{n+m-i-j,\omega_x}} \underbrace{\langle \omega_y \, | i+j \rangle}_{\delta_{i+j,\omega_y}} \\
&= \sum_{i=i_{\min}}^{i_{\max}} (-1)^i \binom{n}{i} \binom{m}{\omega_y - i} \\
&\quad \times c^{\omega_y + n - 2i} s^{\omega_x - n + 2i} \sqrt{\omega_x! \omega_y!}
\end{aligned}
$$

with limits $i_{\min} = \max\{0, n - \omega_x\}$ and $i_{\max} = \min\{\omega_y, n\}$ which are provided by the existence condition of the elements in the sum. Then, the post-selected un-normalized state after the first measurement device can be written as

$$
\begin{aligned}
|\varphi\rangle &= \frac{t^{N+M}}{\sqrt{N!M!}} \left(\frac{r}{t}\right)^{\omega_x + \omega_y} \sqrt{\omega_x! \omega_y!} \qquad \text{(A7)} \\
&\quad \times \sum_{n=\max\{0, \omega_x + \omega_y - M\}}^{\min\{\omega_x + \omega_y, N\}} \binom{N}{n} \binom{M}{\omega_x + \omega_y - n} \\
&\quad \times \sum_{i=i_{\min}}^{i_{\max}} (-1)^i \binom{n}{i} \binom{\omega_x + \omega_y - n}{\omega_y - i} \\
&\quad \times c^{\omega_y + n - 2i} s^{\omega_x - n + 2i} \left(\hat{a}_x^\dagger\right)^{N-n} \left(\hat{a}_y^\dagger\right)^{M - \omega_x - \omega_y + n} |0\rangle,
\end{aligned}
$$

where again the limits in the summation are imposed by the existence conditions of the terms in the sum.

The state above can be written in a clearer and more compact notation as

$$
|\varphi\rangle = \sum_{n=n_{\min}}^{n_{\max}} \mathcal{A}_{n,\mathbf{w}_1}(N, M, \theta, r) | N - n, M + n - \omega_1 \rangle,
$$

(A8)

with multi-index $\mathbf{w}_1 = (\omega_x, \omega_y)$, limits $n_{\min} = \max\{0, \omega_1 - M\}$ and $n_{\max} = \max\{\omega_1, N\}$, where $\omega_1 = \omega_x + \omega_y$ the number of detected photons, and

$$
\begin{aligned}
\mathcal{A}_{n,\mathbf{w}_1}(N, M, \theta, r) &= t^{N+M} \left(\frac{r}{t}\right)^{\omega_1} \binom{N}{n} \binom{M}{\omega_1 - n} \qquad \text{(A9)} \\
&\quad \times \sqrt{\frac{(N-n)!(M+n-\omega_1)! \omega_x! \omega_y!}{N! M!}} \\
&\quad \times \sum_{i=\max\{0, n-\omega_x\}}^{\min\{\omega_y, n\}} (-1)^i \binom{n}{i} \binom{\omega_1 - n}{\omega_y - i} \cos^{\omega_y + n - 2i} \sin^{\omega_x - n + 2i}.
\end{aligned}
$$

Note that although it is not explicitly denoted on its label, $|\varphi\rangle$ depends on all the relevant parameters $(\omega_x, \omega_y, N, M, \theta, r)$.

Being $|\varphi\rangle$ the post-selected un-normalized state after ω_x and ω_y photons are detected, its norm provides the probability $\bar{P}_{\mathbf{w}_1}$ of detecting this number of photons at the first measurement

$$
\bar{P}_{\mathbf{w}_1}(N, M, \theta, r) = \sum_{n=n_{\min}}^{n_{\max}} \left| \mathcal{A}_{n,\mathbf{w}_1}(N, M, \theta, r) \right|^2. \quad \text{(A10)}
$$

From this expression, which is easily computed with the help of a computer, it is simple to find the probability for an a-event in the different types of measurements. For example, for an $\mathcal{S}_\omega$ measurement, we have $P_x = \bar{P}_{(\omega, 0)}$, while for a $\mathcal{B}_{[\omega_{\min}, \omega_{\max}]}$ we have $P_x = \sum_{\omega_x, \omega_y = \omega_{\min}}^{\omega_{\max}} H(\omega_x - \omega_y) \bar{P}_{(\omega_x, \omega_y)}$, where $H(z)$ is the step function defined as 0 for $z \leq 0$ and 1 for $z > 0$.

2. Second measurement

The post-selected state $|\varphi\rangle$ enters a second measurement port with a different orientation θ' of the calcite-crystal axes. We can easily derive the expression of the post-selected state after counting ω_x' and ω_y' photons in the detectors. To this aim, we just note that since $|\varphi\rangle$ is written in the Fock basis as a superposition of $|N', M'\rangle$ states, with $N' = N - n$ and $M' = M + n - \omega_1$, the only thing we need is to find the transformation of these states. It is clear that the transformed $|N', M'\rangle$ will have the same expression as (A8), but replacing N, M, and θ by N', M', and θ', respectively. Hence, the un-normalized transmitted state after the second measurement can be written as

$$
\begin{aligned}
|\varphi'\rangle &= \sum_{n=n_{\min}}^{n_{\max}} \sum_{k=k_{\min}}^{k_{\max}} \mathcal{A}_{n,\mathbf{w}_1}(N, M, \theta, r) \qquad \text{(A11)} \\
&\quad \times \mathcal{A}_{k,\mathbf{w}_1'}(N - n, M + n - \omega_1, \theta', r) \\
&\quad \times | N - k - n, M + k + n - \omega_{12} \rangle,
\end{aligned}
$$

with $\mathbf{w}_1' = (\omega_x', \omega_y')$, limits $k_{\min} = \max\{0, \omega_{12} - n - M\}$ and $k_{\max} = \min\{\omega_1', N - n\}$, and where $\omega_1' = \omega_x' + \omega_y'$ is the number of photons detected in the second measurement, while $\omega_{12} = \omega_x + \omega_y + \omega_x' + \omega_y'$ is the total number of detected photons. Noticing that k and n appear in the states only through the combination $s = n + k$, it is convenient to write $k = s - n$, and change the sum in k by a sum in s, easily arriving at

$$
|\varphi'\rangle = \sum_{s=s_{\min}}^{s_{\max}} \mathcal{B}_{s,\mathbf{w}_2}(N, M, \theta, \theta', r) | N - s, M + s - \omega_{12} \rangle,
$$

(A12)

with $\mathbf{w}_2 = (\omega_x, \omega_y, \omega_x', \omega_y')$, limits $s_{\min} = \max\{0, \omega_{12} - M\}$ and $s_{\max} = \min\{\omega_{12}, N\}$, and

$$
\begin{aligned}
\mathcal{B}_{s,\mathbf{w}_2}(N, M, \theta, \theta', r) &= \sum_{m=m_{\min}}^{m_{\max}} \mathcal{A}_{m,\mathbf{w}_1}(N, M, \theta, r) \\
&\quad \times \mathcal{A}_{s-m,\mathbf{w}_1'}(N - m, M + m - \omega_1, \theta', r),
\end{aligned}
$$

(A13)

with limits $m_{\min} = \max\{0, \omega_1 - M, s - \omega_1'\}$ and $m_{\max} = \min\{\omega_1, N, s\}$.

The un-normalized state $|\varphi'\rangle$ is the post-selected state after ω_x and ω_y photons are detected at the first measurement device, and ω_x' and ω_y' photons are detected at the second measurement device. The corresponding probability $\bar{P}_{\mathbf{w}_2}$ of detecting this number of photons is then given by its norm, which reads

$$\bar{P}_{\mathbf{w}_2}(N, M, \theta, \theta', r) = \sum_{s=s_{\min}}^{s_{\max}} |\mathcal{B}_{s, \mathbf{w}_2}(N, M, \theta, \theta', r)|^2.$$
(A14)

Once we have this bare conditional probabilities for photon counts, we can find the probability P_{ab} of an ab-event for the different type of measurements. In the case of $\mathcal{S}_\omega$ measurements, one easily writes $P_{xx} = \bar{P}_{(\omega, 0, \omega, 0)}$ and $P_{xy} = \bar{P}_{(\omega, 0, 0, \omega)}$, for example. In contrast, considering a more general $\mathcal{B}_{[\omega_{\min}, \omega_{\max}]}$ measurement, we have

$$P_{xx} = \qquad\qquad\qquad\qquad\qquad (A15)$$
$$\sum_{\omega_x, \omega_x' = \omega_{\min}}^{\omega_{\max}} \left(P_{(\omega_x, 0, \omega_x', 0)} + \sum_{\omega_y = \omega_{\min}}^{\omega_x - 1} \sum_{\omega_y' = \omega_{\min}}^{\omega_x' - 1} P_{(\omega_x, \omega_y, \omega_x', \omega_y')} \right.$$
$$+ (1 - \delta_{\omega_x' \omega_{\min}}) \sum_{\omega_y' = \omega_{\min}}^{\omega_x' - 1} P_{(\omega_x, 0, \omega_x', \omega_y')}$$
$$\left. + (1 - \delta_{\omega_x \omega_{\min}}) \sum_{\omega_y = \omega_{\min}}^{\omega_x - 1} P_{(\omega_x, \omega_y, \omega_x', 0)} \right),$$

and

$$P_{xy} = \qquad\qquad\qquad\qquad\qquad (A16)$$
$$\sum_{\omega_x, \omega_y' = \omega_{\min}}^{\omega_{\max}} \left(P_{(\omega_x, 0, 0, \omega_y')} + \sum_{\omega_y = \omega_{\min}}^{\omega_x - 1} \sum_{\omega_x' = \omega_{\min}}^{\omega_y' - 1} P_{(\omega_x, \omega_y, \omega_x', \omega_y')} \right)$$
$$+ \sum_{\omega_x = \omega_{\min}}^{\omega_{\max}} \sum_{\omega_y' = \omega_{\min}+1}^{\omega_{\max}} \sum_{\omega_x' = \omega_{\min}}^{\omega_y' - 1} P_{(\omega_x, 0, \omega_x', \omega_y')}$$
$$+ \sum_{\omega_y' = \omega_{\min}}^{\omega_{\max}} \sum_{\omega_y = \omega_{\min}+1}^{\omega_{\max}} \sum_{\omega_x = \omega_{\min}}^{\omega_y - 1} P_{(\omega_x, \omega_y, 0, \omega_y')}.$$

Similar expressions can be written for the other types of ab-events. These together with the probabilities for the a-events of the previous section are all we need to evaluate correlation functions and LGIs.

3. Third measurement

In order to study no signaling in time, we need to consider a third measurement (characterized by the angle θ'' and a number of detected photons ω_x'' and ω_y''). The derivation follows the same lines we have seen above and the result reads

$$|\varphi''\rangle = \sum_{t=t_{\min}}^{t_{\max}} \mathcal{C}_{t, \mathbf{w}_3}(N, M, \theta, \theta', \theta'', r) \qquad (A17)$$
$$\times |N - s, M + s - \omega_{123}\rangle,$$

with $\mathbf{w}_3 = (\omega_x, \omega_y, \omega_x', \omega_y', \omega_x'', \omega_y'')$, limits $t_{\min} = \max\{0, \omega_{123} - M\}$ and $t_{\max} = \min\{\omega_{123}, N\}$, $\omega_{123} = \omega_x + \omega_y + \omega_x' + \omega_y' + \omega_x'' + \omega_y''$ the total number of detected photons, and

$$\mathcal{C}_{t, \mathbf{w}_3}(N, M, \theta, \theta', \theta'', r) = \sum_{l=l_{\min}}^{l_{\max}} \mathcal{B}_{n, \mathbf{w}_2}(N, M, \theta, \theta', r)$$
(A18)
$$\times \mathcal{A}_{t-l, \mathbf{w}_1''}(N - l, M + l - \omega_{12}, \theta'', r),$$

where $\mathbf{w}_1'' = (\omega_x'', \omega_y'')$, the limits are $l_{\min} = \max\{0, \omega_{12} - M, t - \omega_1''\}$ and $l_{\max} = \min\{\omega_{12}, N, t\}$, and $\omega_1'' = \omega_x'' + \omega_y''$ are the photons detected in the third measurement port.

Finally, we evaluate the probability $\bar{P}_{\mathbf{w}_3}$ of measuring the sequence $\mathbf{w}_3$ of photon numbers as

$$\bar{P}_{\mathbf{w}_3}(N, M, \theta, \theta', \theta'', r) = \sum_{t=t_{\min}}^{t_{\max}} |\mathcal{C}_{t, \mathbf{w}_3}(N, M, \theta, \theta', \theta'', r)|^2.$$
(A19)

From this expression, we can evaluate the probability P_{abc} for an abc-event for the different types of measurements. We don't write the general expressions here because they are too lengthy in the general case, but they are trivially found following the same lines as with ab-events and a-events.

---

[1] A. J. Leggett and A. Garg, Phys. Rev. Lett. **54**, 857 (1985).
[2] C. Emary, N. Lambert, and F. Nori, Rep. Prog. Phys. **77**, 016001 (2014).
[3] A. Palacios-Laloy, F. Mallet, F. Nguyen, P. Bertet, D. Vion, D. Esteve, and A. N. Korotkov, Nat. Phys. **6**, 442 (2010).
[4] A. M. Souza, I. S. Oliveira, and R. S. Sarthour, New J. Phys. **13**, 053023 (2011).
[5] G. C. Knee, S. Simmons, E. M. Gauger, J. J. L. Morton, H. Riemann, N. V. Abrosimov, P. Becker, H.-J. Pohl, K. M. Itoh, M. L.W. Thewalt, G. A. D. Briggs, and S. C. Benjamin, Nat. Commun. **3**, 606 (2012).
[6] A. I. Lvovsky, R. Ghobadi, A. Chandra, A. S. Prasad, and C. Simon, Nature Physics **9**, 541–544 (2013).
[7] A. Asadian, C. Brukner, and P. Rabl, Phys. Rev. Lett. **112**, 190402 (2014).
[8] G. C. Knee, K. Kakuyanagi, M.-C. Yeh, Y. Matsuzaki,

H. Toida, H. Yamaguchi, S. Saito, A. J. Leggett, and W. J. Munro, Nat. Commun. **7**, 13253 (2016).

[9] J. Kofler and C. Brukner, Phys. Rev. A **87**, 052115 (2013).

[10] L. Clemente and J. Kofler, Phys. Rev. Lett. **116**, 150401 (2016).

[11] L. Clemente and J. Kofler, Phys. Rev. A **91**, 062103 (2015).

[12] A. D. Armour, M. P. Blencowe, and K. C. Schwab, Phys. Rev. Lett. **88**, 148301 (2002)

[13] K. C. Schwab and M. L. Roukes, Phys. Today **58**, 36 (2005).

[14] M. Arndt and K. Hornberger, Nat. Phys. **10**, 271 (2014).

[15] M. Abdi, P. Degenfeld-Schonburg, M. Sameti, C. Navarrete-Benlloch, and M. J. Hartmann, Phys. Rev. Lett. **116**, 233604 (2016).

[16] O. Romero-Isart, arXiv:1612.04290.

[17] M. E. Goggin, M. P. Almeida, M. Barbieri, B. P. Lanyon, J. L. O'Brien, A. G. White, and G. J. Pryde, PNAS **108**, 1256 (2011).

[18] J. Kofler and C. Brukner, Phys. Rev. Lett. **99**, 180403 (2007).

[19] T.Wang, R. Ghobadi, S. Raeisi, and C. Simon, Phys. Rev. A **88**, 062114 (2013).

[20] H. Jeong, Y. Lim, and M. S. Kim, Phys. Rev. Lett. **112**, 010402 (2014).

[21] P. Sekatski, N. Gisin, and N. Sangouard, Phys. Rev. Lett. **113**, 090403 (2014).

[22] J. Kofler and C. Brukner, Phys. Rev. Lett. **101**, 090403 (2008).

[23] H. Jeong, M. Paternostro, and T. C. Ralph, Phys. Rev. Lett. **102**, 060403 (2009).

[24] C. Navarrete-Benlloch, *An Introduction to the Formalism of Quantum Information with Continuous Variables* (Morgan & Claypool and IOP, Bristol, 2015).